2026 IEEE/SICE International Symposium on System Integration (SII)
January 11-14, 2026. Cancún, México

A Mobile Robotic Framework for Teleoperated Pipe Inspections in Hydroelectric Power Plants

Guillermo Maldonado, Jabes Guerra, Juan Barrientos, Luis Ayapan and Julio Fajardo

***Abstract*—Hydroelectric power plants constitute the primary source of electricity generation in Guatemala, representing the largest share of the national energy mix, making the inspection and maintenance of infrastructure such as large water inlet pipes (penstocks) crucial. These pipes, which are several kilometers long and have limited access, present hazards for human inspectors. This work introduces a low-cost, modular robotic rover designed for manual inspection of penstocks of varying sizes and conditions. The robot features a tracked locomotion system with an adjustable mechanism for stable alignment and is operated via a web-based joystick interface, enabling real-time anomaly detection. It supports mapping, localization, and data logging for post-inspection analysis. The modular design allows for disassembly and transport through tight spaces, followed by quick reassembly inside the pipe. The rover has successfully conducted multiple inspections in diverse hydroelectric pipelines of different diameters and materials, under diverse sediment accumulation conditions.**

***Index Terms*—Sustainable robotics, renewable and sustainable energy, robot design, integration platforms.**

I. Introduction

According to the Latin American Energy Organization (OLADE), approximately 45.6% of Guatemala's total electrical generation comes from hydroelectric plants [1]. Given this significant contribution to the national energy matrix, it is crucial to ensure the structural integrity and operational safety of hydroelectric infrastructure to maintain reliable power production and distribution [2]–[5]. A vital component of this infrastructure is the network of large water inlet pipes, known as penstocks, which transport high-pressure flows from reservoirs to turbines. These conduits typically extend 2–4 km underground and have internal diameters ranging from (90 to 240 cm), with access limited to a small number of inspection hatches. Conventional inspection methods require human entry into these confined, slippery, and poorly ventilated environments, presenting considerable logistical, safety, and operational challenges. The restricted mobility, low visibility, and potential risks associated with structural hazards make such inspections both inefficient and hazardous. Additionally, the difficulty in accessing the full length of the pipes often leads to incomplete or inconsistent data. Manual inspection processes are inherently time-consuming and prone to human error, especially under adverse environmental conditions. This highlights the urgent need for automated or robotic solutions that can deliver reliable, high-resolution assessments in these complex settings.

In recent years, a variety of robotic and sensor-based solutions have been proposed to minimize human exposure and enhance inspection consistency [6]–[10]. Camera-equipped crawlers and depth-sensing rigs have been utilized for remote visual inspections in municipal water and sewer systems, while 2D and 3D LiDAR technologies have been employed to reconstruct internal pipe geometries and assess deformation. More advanced non-destructive testing (NDT) methods, such as Magnetic Flux Leakage (MFL), have proven effective for detecting fissures and corrosion in steel pipelines [11], [12]; however, they are not applicable to non-ferrous materials like fiberglass-reinforced plastic (FRP), often used in hydroelectric infrastructure. Similarly, commercial solutions are available, such as Fiberscope TROGLOTEK, or Jiutai Technology GT102BPro. However, they require custom cable drums and heavy equipment, which hinders inspection deployment, particularly in rural areas. Despite these advancements, many existing solutions encounter challenges related to multi-material applicability, adaptability to varying diameters, and precise localization over long distances in GPS-denied environments. Numerous inspection robots are designed explicitly for uniform pipelines and lack modularity, complicating deployment in remote locations with restricted access, such as narrow manholes [13]–[15]. Furthermore, confined-space LiDAR and stereo-vision mapping face unique challenges in cylindrical geometries, including repetitive features, data sparsity, and occlusions caused by water or debris.

To address the operational and safety challenges associated with inspecting hydroelectric penstocks and similar confined structures, this work proposes a robotic inspection system utilizing a rubber-tracked rover, as depicted in Fig. 1. This robot is equipped with a tracked locomotion platform and a web-based supervisory interface, allowing for operation both locally and remotely. Its mechanical design can accommodate variations in pipe diameter, longitudinal slopes, and diverse surface conditions, ensuring it maintains mobility and stability under various environmental constraints. The rover operates exclusively in teleoperation mode, with a trained inspection operator controlling the platform via a joystick. Due to the characteristics of the inspection environment, consisting of a continuous downward slope, slippery surfaces caused by sediment accumulation, and the stabilizing effect of the rover's weight, combined with its adjustable track

Author is with Turing Research Laboratory, FISICC, Galileo University, Guatemala City, Guatemala. julio.fajardo@galileo.edu

978-1-6654-5784-2/26/$31.00 ©2026 IEEE

Fig. 1. Side view of the modular pipe inspection rover, with LiDAR and side cameras mounted.

mechanism, autonomous centering control is unnecessary, as the platform naturally remains aligned within the conduit. This operational approach also allows the operator to decide which areas to inspect in detail directly and to focus on potential anomalies as they are identified during the inspection. Onboard computing resources enable real-time localization and mapping, allowing for precise assessments of structural damage, deformations, and obstructions. Additionally, all inspection data is logged and stored for later analysis and reporting. The modular design of the rover consists of separable units that handle control (including embedded computing, sensing, and communication) and locomotion/power (such as batteries, motors, and drive systems). This design facilitates disassembly for transport through restricted access points and allows for quick reassembly within the inspection environment. Overall, this configuration enhances deployment flexibility while balancing cost, performance, and operational robustness.

The remainder of this paper is organized as follows: Section II describes the proposed solution, integration process, and implementation. Section III presents experimental results and field deployment outcomes. Finally, Section IV summarizes the conclusions and outlines future work.

II. Methods

The robot is structured into two modular subsystems specifically engineered to enhance transportation to the inspection site and facilitate insertion and assembly in confined spaces. The lower module encompasses the locomotion mechanism, lithium-ion battery storage (22.2 V, 15 Ah for logic and 18.5 V, 39 Ah for motors), a Roboteq MDC2460 motor controller, and a Roboteq BMS1040A battery management system. This configuration ensures precise drive control and robust power regulation, contributing to extended operational endurance. In contrast, the upper module contains the embedded computing and sensing systems. It features an NVIDIA® Jetson AGX Xavier computer, along with a 4-Port PCI Express SuperSpeed USB 3.0 controller card that interfaces with three RGB-D cameras. Additionally, this module includes a Gigabit Fiber Optical Media Converter (1000/100 Mbps Ethernet), an Ethernet switch that interfaces with a Velodyne LiDAR with its dedicated interface module, and two DC–DC step-down converters that provide 18 V and 12 V to various subsystems. Both modules are electrically interconnected by a custom cable that transmits power and communication signals, facilitating seamless integration between the embedded computer and the Roboteq control modules. The rover communicates with the operator through a long-range fiber optic link, enabling real-time control via a web-based interface. The following subsections will provide a comprehensive description of the system's core functionalities: locomotion, Simultaneous Localization and Mapping (SLAM), data acquisition and processing, web interface operation, and automated inspection report generation.

A. Locomotion

The rover utilizes a differential tracked locomotion system that features two parallel rubber tracks, each powered by an independent 18 V brushed DC motor paired with a high-ratio planetary gearbox (1260:1), including the sprocket gear ratio. This setup is further connected to a three-stage right-angle gearbox shown in Fig. 2. As a result, the transmission delivers an output shaft speed of approximately 15 rpm and sufficient nominal torque, ensuring reliable operation over uneven and high-resistance terrain. The tracked mechanism can be manually adjusted to fit three different ranges of pipe diameters: 90–100 cm, 150–160 cm, and greater than 240 cm, as shown in Fig. 2. This adaptability allows the rover to optimize its stance and track spacing for enhanced traction and stability across various inspection environments. Weighing approximately 45.4 kg, the rover benefits from a low center of gravity and sufficient downward force, enabling it to maintain a stable path along the central axis of the pipe without the need for active centering control. This inherent stability is further supported by the characteristics of the

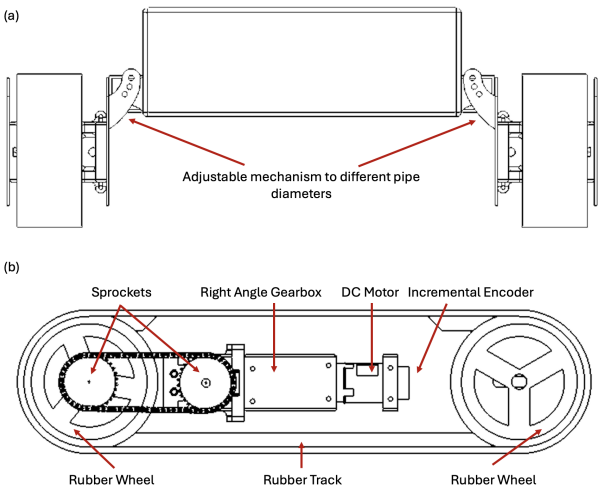

Fig. 2. (a) Detailed mechanical design of the rover's adjustable track mechanism, highlighting components that allow adaptation to different pipe diameters. (b) Side view of the rubber track assembly, illustrating the track layout and contact interface with the pipe surface.

inspection environment, where continuous slopes and slippery surfaces resulting from accumulated sediment naturally guide the platform to stay aligned with the conduit's centerline during operation. Furthermore, each motor is equipped with an incremental rotary encoder with a resolution of 1024 pulses per revolution (PPR), enabling fine velocity and position control by providing high-resolution feedback on shaft position and rotational velocity. This data is processed by an intelligent motor driver that implements closed-loop speed and position control, allowing for precise regulation of forward motion and traveled distance, as depicted in Fig. 2. The motor driver communicates with the onboard computing unit, a NVIDIA Jetson running Ubuntu 22.04 LTS, through a USB serial interface. The control architecture is designed using the Robot Operating System (ROS) Noetic [16], which offers a flexible and modular framework. It integrates specialized nodes for perception, navigation, and decision-making. This architecture facilitates seamless real-time command transmission, continuous monitoring of the system, and thorough data logging during field operations, thereby enhancing operational reliability and supporting comprehensive post-mission analysis.

B. Perception System

The sensors mounted on the upper module (as illustrated in Fig. 1) consist of two Intel RealSense D455 RGB-D cameras positioned on either side (each equipped with a high-intensity LED floodlight), one Intel RealSense D435i camera facing the front of the robot, and a Velodyne VLP-16 LiDAR sensor that is angled at 45° to optimize the detection of the pipe floor. The front camera provides the operator with a real-time overview of the robot's path, allowing for the monitoring of potential flooding from water or sediment, as well as the identification of obstacles that the robot cannot navigate. On the other hand, the side cameras are primarily utilized for visual inspection tasks, enabling the operator to detect surface anomalies along the pipe and examine the joints between segments. These cameras also gather data for 3D reconstruction of the pipe's interior, which supports detailed mapping and documentation efforts [17]. The orientation of the LiDAR sensor helps to reduce point cloud loss that can occur due to large pipe diameters and the sensor's limited vertical field of view, thus preventing central scan lines from projecting into empty space rather than capturing the pipe surface. The onboard computing module processes data from all sensors to create maps for inspection and localization purposes.

C. Data Acquisition & Processing

LiDAR and depth sensors capture intricate 3D point clouds and visual data of the penstock interior. At the same time, the IMU (integrated in RealSense cameras), and rotary encoders deliver precise motion and odometry information. Both HDL Graph SLAM and RTAB-Map techniques were employed to generate these maps, ensuring robust identification and

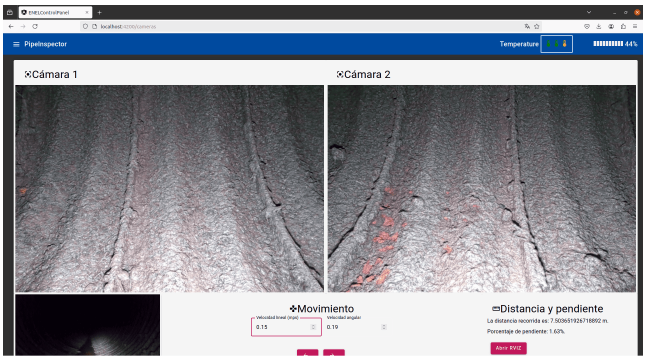

Fig. 3. Web interface showing live feed from two cameras (left & right) and front camera (bottom left). Navigation and movement data is shown as well (bottom center and bottom right, respectively. Temperature and battery status are displayed in the upper right corner.

localization of potential anomalies within designated environments [18], [19]. As a result, the robot's position is determined not only through dead-reckoning based on rotary encoder odometry but also by fusing odometry information with the spatial maps produced by these SLAM methods, thereby enhancing overall mapping accuracy and reliability [13]. This combination facilitates location-aware three-dimensional measurements of critical structural features, including pipe joints, fissure dimensions, and other geometric elements pertinent to inspection [20]. The LiDAR data are crucial for detecting and quantifying pipe deformation, such as ovality and eccentricity resulting from external pressures or soil loads, as well as for identifying potential anomalies along the pipe surface [21], [22]. Concurrently, the RGB-D cameras reconstruct the interior surfaces of the pipe, generating dense 3D models that allow for accurate measurement of relevant Euclidean distances and spatial relationships [17]. Additionally, the front camera's integrated IMU is used to estimate the slope percentage [23], [24].

D. Web Based Interface and Automatic Report Generation

A web-based application, illustrated in Fig. 3, was developed using the Angular framework to provide a comprehensive interface for interacting with the robotic platform, leveraging the rosbridge_suite WebSocket server for seamless communication with ROS nodes [25], [26]. The application displays real-time data streams, including 2D video feeds from the onboard cameras, three-dimensional point clouds generated by both the Velodyne LiDAR sensor and the Intel RealSense depth cameras, and live telemetry from the motor drivers, such as current, voltage, linear displacement, robot pose, and encoder readings. The interface also includes dynamic visualization tools (such as shortcut to open RViz) and diagnostic panels that allow the operator to monitor system status and performance metrics at a glance [27]. Rover control is executed in real time via a Bluetooth-connected joystick, enabling the operator to maneuver the platform precisely within confined and potentially hazardous environments, providing a flexible, platform-independent control and

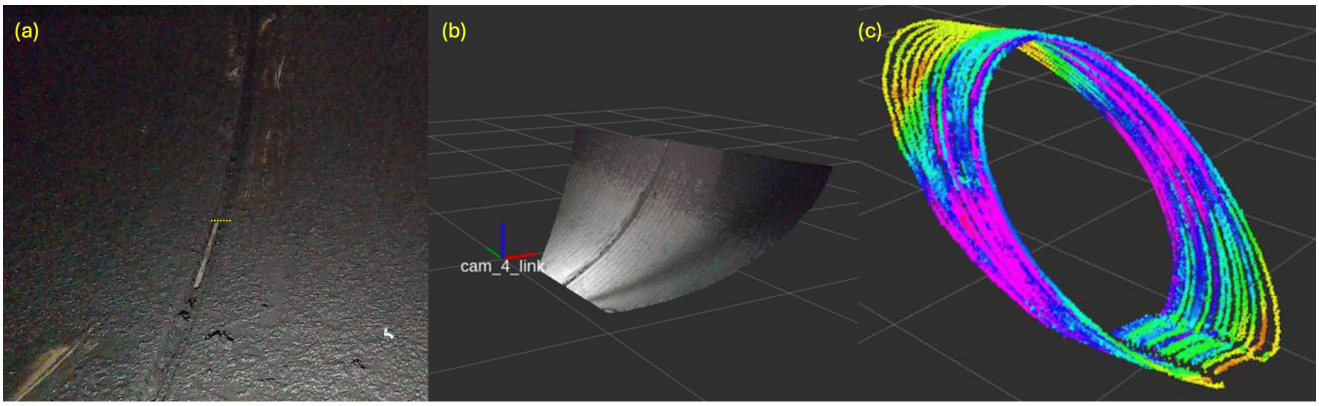

Fig. 4. Visual inspection and reconstruction of the interior of a pipeline under real operating conditions. (a) Operator's camera view during field inspection, showing the inner wall of the pipe with sediment accumulation and a visible junction. (b) 3D reconstruction of the cleaned pipe section after maintenance, where the junction can be clearly observed. (c) Point cloud representation of the inspected pipeline, providing complete surface coverage and highlighting the pipe's inclination along its axis, as well as a potential obstacle or anomaly on the floor.

monitoring system that supports both local and remote operation. In this way, it facilitates rapid decision-making from the operators during inspections and ensures that data acquisition is synchronized and logged for subsequent analysis and reporting. Inspect data are visualized in real time through a web-based interface, allowing the operator to review sensor feeds, telemetry, and reconstructed 3D models of the pipe interior. In this way, the operator has the ability to selectively mark or annotate relevant information, such as detected anomalies, deformations, or structural measurements, to be incorporated into the inspection findings. Once the review is finalized, the system automatically compiles all approved data into a standardized PDF report, which includes quantitative measurements, annotated images, 3D visualizations, and pertinent telemetry. This automated reporting process ensures consistency, minimizes human error, and streamlines documentation workflows. The generated report can be securely archived in a digital database, providing a reliable reference for future inspections, maintenance planning, and compliance verification, while also facilitating the traceability of previously identified anomalies and structural assessments.

Fig. 5. Validation test in a controlled environment, consisting of a 12 meter fiberglass pipe segment with a 1.5 meter diameter, free of sediment.

III. Results

The rover illustrated in Fig. 1 was meticulously designed, fabricated, and subjected to rigorous testing before its successful deployment for inspection missions within the inlet pipes of three hydroelectric power plants, each featuring distinct pipe diameters. During these operations, the integrated multi-sensor subsystem, including LiDAR, RGB-D cameras, an integrated IMU, and wheel encoders, captured high-fidelity geometric and positional data. These results enabled accurate three-dimensional reconstructions of the inspected pipe sections. From these reconstructions, advanced processing algorithms computed ovality indices to quantify structural deformation, measured joint thickness to detect potential misalignments or separations, and extracted spatial metrics to characterize fissures and other irregularities. Complementary field results are illustrated in Fig. 4, the picture on the left, captures the operator's perspective during an actual inspection, showcasing sediment accumulation and visible junctions. Fig. 4(b), a three-dimensional reconstruction of the cleaned pipe section post-maintenance is displayed, with the junction identifiable; this is particularly useful to measure Euclidean distances and sizes of possible anomalies. Fig. 4(c) features a point cloud representation that offers complete surface coverage, highlighting the pipe's inclination as well as potential obstacles or anomalies along the pipe floor, which is also helpful to estimate pipe deformation and ovality index.

The results highlight the robot's ability to perform reliable in-situ inspections and deliver comprehensive structural diagnostics in complex hydroelectric systems. Prior to the actual field inspection, each subsystem was individually tested and validated in replacement pipe segments and in indoor controlled environments, avoiding posed risks from the operator's side. These evaluations included a test for the accuracy of joint thickness measurements, which was assessed in a controlled laboratory experiment: four male volunteers (ages 23 to 41) without prior knowledge of the ground truth were asked to measure five different simulated pipe joints using the proposed tool. The values obtained showed an average

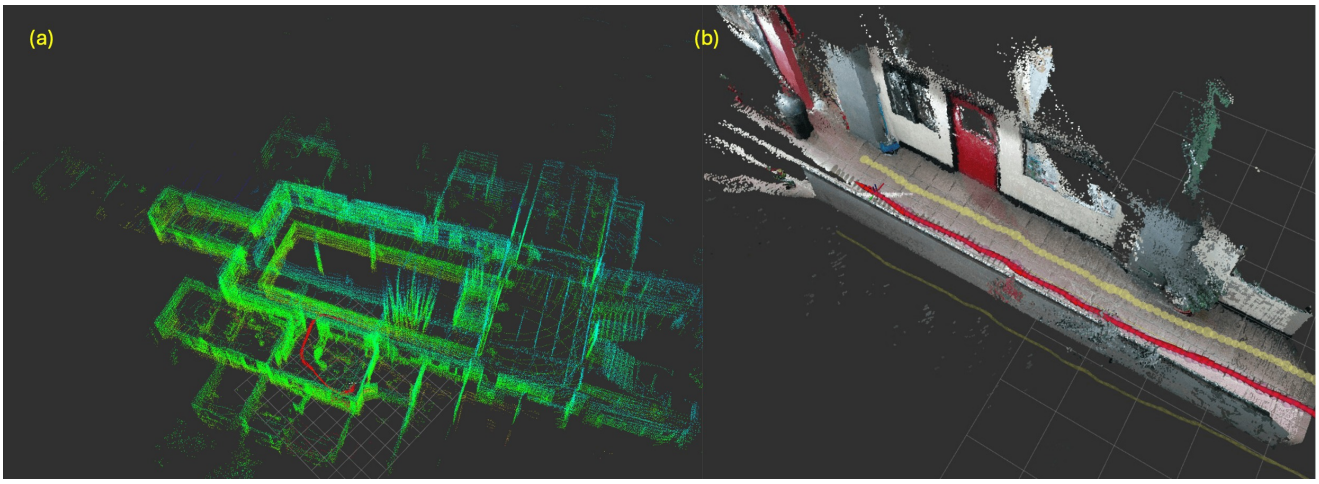

Fig. 6. Results of SLAM experiments conducted in controlled indoor environments. (a) HDL Graph SLAM reconstruction based on LiDAR data, showing a dense and consistent 3D point cloud map with the red line indicating the estimated odometry trajectory. (b) RTAB-Map SLAM reconstruction based on RGB-D camera data, where the red line corresponds to odometry and the environment is accurately reconstructed with detailed visual features. Both approaches demonstrate satisfactory performance under controlled conditions, providing a baseline for subsequent evaluations in penstock inspection scenarios.

error of approximately $4.37\% \pm 0.77\%$ compared to the actual dimensions, confirming that the method provides a reliable estimate of the joint size for practical inspection tasks. The pipe ovality percentage was tested along one replacement pipe segment with a diameter of approximately 2.4 meters, resulting in an error less than $2\% \pm 0.15\%$.

The validation of the complete system took place in two different environments: controlled trials on spare pipe segments, where runs of up to 12 meters were conducted, as demonstrated in Fig. 5, and real inspection scenarios inside the underground inlet pipes, where the rover successfully traversed distances ranging from 50 to 150 meters. The penstocks are large underground conduits that were completely drained for safe robotic inspection. The rover was inserted through dedicated inspection and maintenance holes and then navigated along the pipe's interior, where its adjustable traction mechanism demonstrated reliable adaptation to the varying diameters and surface conditions. Furthermore, the system generated a spatial occupancy map by fusing multi-modal 3D sensor data, which not only facilitated detailed reporting but also enabled the longitudinal monitoring of pipe integrity across successive inspections. To improve localization and mapping accuracy, experiments were carried out using HDL Graph SLAM, which has better performance than some alternatives [28], and RTAB-Map SLAM (which showed better overall accuracy on simulation tests in [29]), both of which were integrated with dead-reckoning odometry. These trials showed satisfactory results in controlled indoor environments. Representative results are presented in Fig. 6, where the red line depicts the odometry trajectory, the HDL Graph SLAM reconstruction (LiDAR-based) is shown on the left, and the RTAB-Map SLAM reconstruction (RGB-D-based) is displayed on the right.

IV. Conclusion

This work introduces a modular robotic framework designed for teleoperated penstock inspection in hydroelectric power plants, successfully implemented in real operational environments. By integrating LiDAR, RGB-D cameras, IMU, and encoder-based odometry, the system enables precise 3D reconstructions of inspected pipe segments, facilitating structural assessment through measurements of ovality, joint thickness, and fissures. A key aspect of the proposed system is its ability to operate in real time under teleoperation via a fiber optic communication link, which ensures both reliable data transmission and the safety of inspection personnel. This capability allows operators to remotely visualize the internal status of the pipes as the mission unfolds, enabling immediate assessment of conditions without exposing humans to hazardous environments. In addition, the system supports the acquisition of precise in-situ measurements of structural and geometric features of interest, which can be directly incorporated into an automatically generated PDF report. All findings are simultaneously stored in a dedicated database, ensuring a traceable record of inspection events and facilitating longitudinal studies by enabling future retrieval and comparative analysis. This comprehensive workflow not only enhances operational safety but also provides hydroelectric companies with a robust tool for long-term infrastructure monitoring and decision-making.

Despite these advancements, the findings underscore the need for further enhancement of odometry and SLAM methodologies. In practical settings, the system often operates in featureless environments akin to the long-corridor problem, where the lack of distinctive landmarks limits loop closure opportunities and exacerbates drift. Although experiments utilizing HDL Graph SLAM and RTAB-Map SLAM in conjunction with dead-reckoning odometry have yielded satisfactory results under controlled indoor conditions, additional refinement and algorithmic improvements

are necessary to achieve similar reliability within hydroelectric conduits under actual operating conditions. On the other hand, the incorporation of deep learning techniques, particularly foundation models and diffusion models, presents promising potential for the autonomous detection of structural anomalies such as fissures, deformations, and obstacles. Nonetheless, the ultimate responsibility for confirming whether a detected feature represents a true anomaly must rest with the trained inspection operator. This requirement reinforces the current framework's reliance on teleoperation, as the high-stakes nature of inspection necessitates qualified human oversight for critical decisions involving safety and costs. Finally, it is essential to highlight the considerable economic and human benefits that robotic inspections can offer in hydroelectric environments. The confined and hazardous conditions of penstock settings, coupled with the pollution affecting numerous rivers in Latin America, create significant risks for manual inspections, rendering them both unsafe and unsustainable. In this way, it is crucial to prioritize the health and safety of inspection personnel who navigate these challenging circumstances.

ACKNOWLEDGMENT

The authors extend their sincere gratitude to Enel Green Power Energy Centroamerica for their support and collaboration, which made this project possible.

REFERENCES

[1] Organización Latinoamericana de Energía (OLADE), "Panorama energético de américa latina y el caribe 2024," Informe anual, OLADE, 2024. [Online]. Available: https://www.olade.org/publicaciones/panorama-energetico-de-america-latina-y-el-caribe-2024/

[2] A. Adamkowski, "Case study: Lapino powerplant penstock failure," *Journal of hydraulic engineering*, vol. 127, no. 7, pp. 547–555, 2001.

[3] O. Fecarotta, C. Arico, A. Carravetta, R. Martino, and H. M. Ramos, "Hydropower potential in water distribution networks: Pressure control by pats," *Water resources management*, vol. 29, no. 3, pp. 699–714, 2015.

[4] A. Göksenli and B. Eryürek, "Failure analysis of pipe system at a hydroelectric power plant," *World Academy of Science, Engineering and Technology, International Journal of Mechanical, Aerospace, Industrial, Mechatronic and Manufacturing Engineering*, vol. 9, no. 9, pp. 1643–1646, 2015.

[5] J. Singh, S. Singh, and J. P. Singh, "Investigation on wall thickness reduction of hydropower pipeline underwent to erosion-corrosion process," *Engineering Failure Analysis*, vol. 127, p. 105504, 2021.

[6] I. N. Ismail, A. Anuar, K. S. M. Sahari, M. Z. Baharuddin, M. Fairuz, A. Jalal, and J. M. Saad, "Development of in-pipe inspection robot: A review," in *2012 IEEE Conference on Sustainable Utilization and Development in Engineering and Technology (STUDENT)*, 2012, pp. 310–315.

[7] P. Ridao, M. Carreras, D. Ribas, and R. Garcia, "Visual inspection of hydroelectric dams using an autonomous underwater vehicle," *Journal of Field Robotics*, vol. 27, no. 6, pp. 759–778, 2010.

[8] P. Ambati, K. S. Raj, and A. Joshuva, "A review on pipeline inspection robot," in *AIP Conference Proceedings*, vol. 2311, no. 1. AIP Publishing LLC, 2020, p. 060002.

[9] B. John and M. Shafeek, "Pipe inspection robots: a review," in *IOP Conference Series: Materials Science and Engineering*, vol. 1272, no. 1. IOP Publishing, 2022, p. 012016.

[10] A. Verma, A. Kaiwart, N. D. Dubey, F. Naseer, and S. Pradhan, "A review on various types of in-pipe inspection robot," *Materials Today: Proceedings*, vol. 50, pp. 1425–1434, 2022.

[11] A. N. Chand, N. Zuhdi, A. Mansor, A. Iqbal, F. Rustam, and W. Baur, "An industrial robot for firewater piping inspection and mapping," in *2021 IEEE/RSJ International Conference on Intelligent Robots and Systems (IROS)*. IEEE, 2021, pp. 2337–2344.

[12] K.-W. Jeon, E.-J. Jung, J.-H. Bae, S.-H. Park, J.-J. Kim, G. Chung, H.-J. Chung, and H. Yi, "Development of an in-pipe inspection robot for large-diameter water pipes," *Sensors*, vol. 24, no. 11, p. 3470, 2024.

[13] J. M. Aitken, M. H. Evans, R. Worley, S. Edwards, R. Zhang, T. Dodd, L. Mihaylova, and S. R. Anderson, "Simultaneous localization and mapping for inspection robots in water and sewer pipe networks: A review," *IEEE access*, vol. 9, pp. 140 173–140 198, 2021.

[14] S. Kazeminasab, N. Sadeghi, V. Janfaza, M. Razavi, S. Ziyadidegan, and M. K. Banks, "Localization, mapping, navigation, and inspection methods in in-pipe robots: A review," *IEEE access*, vol. 9, pp. 162 035–162 058, 2021.

[15] O. O. Emmanuel, M. J. Salami, and R. O. Lawan, "A comprehensive review of autonomous navigation systems for in-pipe inspection robots using advanced slam techniques," in *2024 IEEE 5th International Conference on Electro-Computing Technologies for Humanity (NIGERCON)*. IEEE, 2024, pp. 1–5.

[16] M. Quigley, K. Conley, B. Gerkey, J. Faust, T. Foote, J. Leibs, R. Wheeler, A. Y. Ng *et al.*, "Ros: an open-source robot operating system," in *ICRA workshop on open source software*, vol. 3, no. 3.2. Kobe, 2009, p. 5.

[17] K. A. Tychola, I. Tsimperidis, and G. A. Papakostas, "On 3d reconstruction using rgb-d cameras," *Digital*, vol. 2, no. 3, pp. 401–421, 2022.

[18] K. Koide, J. Miura, and E. Menegatti, "A portable three-dimensional lidar-based system for long-term and wide-area people behavior measurement," *International Journal of Advanced Robotic Systems*, vol. 16, no. 2, p. 1729881419841532, 2019.

[19] M. Labbé and F. Michaud, "Rtab-map as an open-source lidar and visual simultaneous localization and mapping library for large-scale and long-term online operation," *Journal of field robotics*, vol. 36, no. 2, pp. 416–446, 2019.

[20] E. Lachat, H. Macher, T. Landes, and P. Grussenmeyer, "Assessment and calibration of a rgb-d camera (kinect v2 sensor) towards a potential use for close-range 3d modeling," *Remote Sensing*, vol. 7, no. 10, pp. 13 070–13 097, 2015.

[21] P. Schalk, R. Ofner, and P. O'Leary, "Pipe eccentricity measurement using laser triangulation," *Image and Vision Computing*, vol. 25, no. 7, pp. 1194–1203, 2007.

[22] H. Zou, R. Xia, Y. Zeng, J. Zhao, Y. Chen, T. Zhang, T. Zhang, and S. Fu, "Ovality measurement based on scanning point cloud for tube bend deformation analysis," *The International Journal of Advanced Manufacturing Technology*, vol. 125, no. 7, pp. 3743–3760, 2023.

[23] M. Kamal Mazhar, M. J. Khan, A. I. Bhatti, and N. Naseer, "A novel roll and pitch estimation approach for a ground vehicle stability improvement using a low cost imu," *Sensors*, vol. 20, no. 2, p. 340, 2020.

[24] M. L. Hoang and A. Pietrosanto, "New artificial intelligence approach to inclination measurement based on mems accelerometer," *IEEE Transactions on Artificial Intelligence*, vol. 3, no. 1, pp. 67–77, 2021.

[25] M. Blaha, M. Krec, P. Marek, T. Nouza, and T. Lejsek, "Rosbridge web interface," *Department of Cybernetics Faculty of Electrical Engineering, Czech Technical University Technick*, vol. 166, p. 27, 2013.

[26] C. Crick, G. Jay, S. Osentoski, B. Pitzer, and O. C. Jenkins, "Rosbridge: Ros for non-ros users," in *Robotics research: The 15th international symposium ISRR*. Springer, 2016, pp. 493–504.

[27] H. R. Kam, S.-H. Lee, T. Park, and C.-H. Kim, "Rviz: a toolkit for real domain data visualization," *Telecommunication Systems*, vol. 60, no. 2, pp. 337–345, 2015.

[28] I. Filip, J. Pyo, M. Lee, and H. Joe, "Lidar slam comparison in a featureless tunnel environment," in *2022 22nd International Conference on Control, Automation and Systems (ICCAS)*. IEEE, 2022, pp. 1648–1653.

[29] K. J. De Jesus, H. J. Kobs, A. R. Cukla, M. A. d. S. L. Cuadros, and D. F. T. Gamarra, "Comparison of visual slam algorithms orb-slam2, rtab-map and sptam in internal and external environments with ros," in *2021 Latin American Robotics Symposium (LARS), 2021 Brazilian Symposium on Robotics (SBR), and 2021 Workshop on Robotics in Education (WRE)*. IEEE, 2021, pp. 216–221.